GEOPHYSICAL RESEARCH LETTERS, VOL. 35, L16602, doi:10.1029/2008GL035058, 2008

Semiannual variation in the western tropical Pacific Ocean

Tangdong Qu,[1] Jianping Gan,[2] Akio Ishida,[3] Yuji Kashino,[3] and Tomoki Tozuka[4]

Received 18 June 2008; accepted 18 July 2008; published 28 August 2008.

[1] Analysis of altimeter data combined with results from a high-resolution general circulation model has revealed the existence of a semiannual variation in the western tropical Pacific. The semiannual variation cannot be explained by local Ekman pumping alone, but is also related to the westward propagation of Rossby waves originating in the central tropical Pacific, corresponding in the northern hemisphere with the Inter-Tropical Convergence Zone and in the southern hemisphere with the South Pacific Convergence Zone. This signal intensifies toward the western boundary and appears to have a notable impact on the circulation there. In the Mindanao Current, the semiannual variation is of comparable strength with the annual variation. This finding is supported by a moored acoustic Doppler current profile measurement during the period from October 1999 to July 2002. **Citation:** Qu, T., J. Gan, A. Ishida, Y. Kashino, and T. Tozuka (2008), Semiannual variation in the western tropical Pacific Ocean, *Geophys. Res. Lett.*, *35*, L16602, doi:10.1029/2008GL035058.

1. Introduction

[2] The North Equatorial Current (NEC) bifurcates, as it approaches the Philippine coast, into the northward flowing Kuroshio and southward-flowing Mindanao Current (MC) [e.g., *Nitani*, 1972; *Qu and Lukas*, 2003]. The MC continues southward to feed the North Equatorial Countercurrent (NECC), forming a highly variable current system in the western tropical Pacific. This current system is linked to a cold, cyclonic circulation, often referred to as the Mindanao Dome [e.g., *Masumoto and Yamagata*, 1991], and appears to be climatologically important, among other things being closely related to the Asian monsoon and El Nino/Southern Oscillation [e.g., *Lukas et al.*, 1991; *Tozuka et al.*, 2002].

[3] Studies of the NEC-MC-NECC current system have focused on its seasonal to interannual variations [e.g., *Lukas*, 1988; *Toole et al.*, 1990; *Mitchum and Lukas*, 1990; *Wijffels et al.*, 1995; *Qu et al.*, 1998; *Masumoto and Yamagata*, 1991; *Tozuka et al.*, 2002; *Kashino et al.*, 2001, 2005]. Due to the paucity of observations, however, our understanding of these variations is far from complete. The rapid advance in space-based remote sensing allows a fresh look at this problem. Analysis of altimeter data, for example, provides a broad, consistent view of seasonal variation over the entire tropical Pacific (Figure 1). In the northern hemisphere, the seasonal variation of sea surface height (SSH) is dominated by the annual cycle. Two maxima (>10 cm) can be seen in amplitude of the annual cycle (Figure 1a), one lying between 120°W and 160°W at about 5°N and the other between 140°W and 100°W at about 10°N (Figure 1a). These maxima have been studied in literature and can be attributed in a large part to the local Ekman pumping [e.g., *Wang et al.*, 2000; *Kessler*, 2006]. A secondary maximum (>6 cm) is seen in the Philippine Sea, consistent with the annual migration of NEC bifurcation stemming from the seasonally reversing monsoon [e.g., *Qu and Lukas*, 2003].

[4] The SSH in the tropical Pacific also exhibits a semiannual variation (Figure 1b), though its amplitude is somewhat smaller. The semiannual variation is confined within about 5° of the equator, corresponding in the northern hemisphere with the Inter-Tropical Convergence Zone (ITCZ) and in the southern hemisphere with the South Pacific Convergence Zone (SPCZ). This signal intensifies toward the western boundary, with its maximum amplitude exceeding 4 cm near 5°N. Although the semiannual variation along the 4°–6°N wave band was previously noticed [e.g., *Kessler*, 1990; *Wang et al.*, 2000], its dynamics and impact on the western boundary current have not been carefully examined. This study addresses this issue using altimeter data combined with results from a high-resolution ocean general circulation model (GCM).

2. Origin of the Semiannual Variation

[5] Circulation in the upper kilometer of the tropical ocean is primarily wind driven. To identify the origin of semiannual variation in the western tropical Pacific, we examine the climatological wind products from the European Remote Sensing (ERS) satellite microwave scatterometer measurements. The ERS data span from August 1991 to January 2001, covering almost the same period as the merged SSH measurements (January 1993–December 2005) described above. Harmonic analysis of the ERS downward Ekman pumping velocity shows two maximum annual variations in the central tropical Pacific (Figure 1c). One lies around 10°N, with its amplitude exceeding 3×10^{-4} cm s^{-1} at 140°W–160°W, approximately coinciding with the large annual variation in the SSH (Figure 1a). The other is confined within about 5° of the equator, reflecting the dominance of planetary beta effect near the equator. The annual variation in downward Ekman pumping is also large (>6×10^{-4} cm s^{-1}) in the far western tropical Pacific, being primarily responsible for the annual variation in SSH [*Mitchum and Lukas*, 1990; *Masumoto and Yamagata*, 1991].

[1] International Pacific Research Center, SOEST, University of Hawai'i at Mānoa, Honolulu, Hawaii, USA.
[2] Department of Mathematics and Atmospheric, Marine and Coastal Environment Program, Hong Kong University of Science and Technology, Hong Kong, China.
[3] Japan Agency for Marine-Earth Science and Technology, Yokosuka, Japan.
[4] Department of Earth and Planetary Science, Graduate School of Science, University of Tokyo, Tokyo, Japan.

0094-8276/08/2008GL035058$05.00

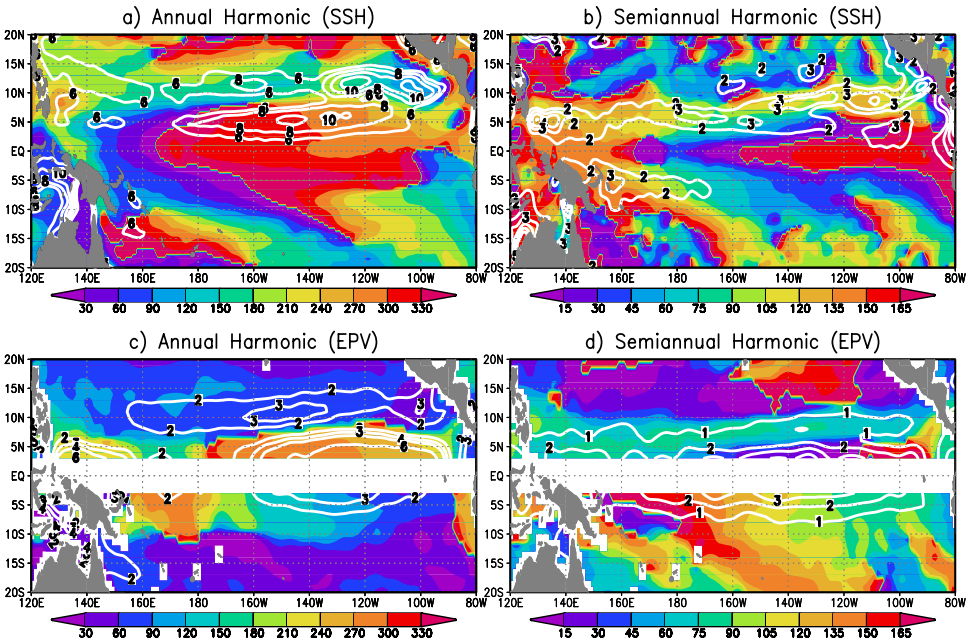

Figure 1. (left) Annual and (right) semiannual harmonics of (top) the merged TOPEX/Poseidon, ERS, and Jason1 sea surface height (cm) climatology and (bottom) the ERS downward Ekman pumping velocity (10^{-4} cm s^{-1}) climatology. The contours represent amplitude, and the colors denote phase of the harmonics, corresponding to the day of the calendar year.

[6] The semiannual variation in downward Ekman pumping is largest (>3 × 10^{-4} cm s^{-1}) near the equator (Figure 1d), for the same reason as discussed for the annual variation. A secondary maximum (>1 × 10^{-4} cm s^{-1}) is seen extending across the tropical Pacific along about 5°N, approximately coinciding with the maximum semiannual variation in SSH (Figure 1b), as well as in precipitation associated with the ITCZ (figure not shown). In the far western tropical Pacific, the semiannual variation in Ekman pumping does not show a consistent pattern with that in SSH (Figure 1b). Apparently, the maximum semiannual variation (>4 cm) in SSH there cannot be accounted for by local Ekman pumping alone.

[7] Large-scale, low-frequency variation in SSH is forced not only by local Ekman pumping, but also by the propagation of Rossby waves from the east [e.g., *Meyers*, 1979; *Kessler*, 1990, 2006]. At 5°N, the annual Rossby waves are forced by downward Ekman pumping in the eastern tropical Pacific (∼120°W) in September/October (Figure 2). These waves propagate westward and reach the international dateline in about 3 months. In a similar way, the semiannual Rossby waves are forced by downward Ekman pumping in the eastern tropical Pacific (∼120°W) twice a year, one in June/July and the other in December/January. The mean westward phase speed of these waves is about 0.8 m s^{-1} (Figure 3), consistent with the theoretical phase speed of the first baroclinic Rossby waves [e.g., *Kessler*, 1990, 2006; *Wang et al.*, 2000].

[8] Careful examination of time-longitude variations shows an obvious discontinuity in propagation around the international dateline (Figure 2). To the east, the westward propagating signal in SSH is nearly in phase with local Ekman pumping (Figure 3), but the former has a maximum variation extending farther westward by 20°–40° than the latter (Figure 2). This result seems to suggest that the westward propagating signal in SSH is a Rossby wave continuously forced by the local Ekman pumping applied over it. The propagating signal in local Ekman pumping disappears west of the dateline. On the annual time scale, the downward Ekman pumping is maximum in July/August and minimum in January/February (Figure 2), and on the semiannual time scales, the downward Ekman pumping approaches its maxima in March and September. Both variations are consistent with the seasonal migration of monsoon [*Wang et al.*, 2000].

[9] The westward propagating signal is evident in SSH across the entire tropical Pacific (Figure 3). Near the international dateline, as already noted in literature [e.g., *Tozuka et al.*, 2002], the downward Ekman pumping maximum (>3 × 10^{-4} cm s^{-1}) generates a downwelling Rossby wave in January/February near 5°N (Figure 3c). As this downwelling Rossby wave arrives at 140°–160°E in spring, the Mindanao Dome quickly diminishes. The large degree of cancellation between local Ekman pumping and the westward propagation of Rossby waves results in a weaker annual variation in the western tropical Pacific (Figures 2b and 3a) than in the east. The semiannual variation also shows a westward propagating signal in SSH (Figure 3c). Near the dateline, the two maxima occur in April and October, approximately during the transition seasons of monsoon when Ekman pumping velocity changes sign. As we progress westward, the maximum SSH tends to occur in a later date. The phase speed of the semiannual westward propagation is significantly faster than that in the east. Apparently, the Rossby waves emanating from east of the dateline are strongly modified by local Ekman pumping associated with monsoon. For example, when downward Ekman pumping reaches its maximum in March, it generates downwelling Rossby waves at different longitudes of the western tropical Pacific (130°E–180°). These waves

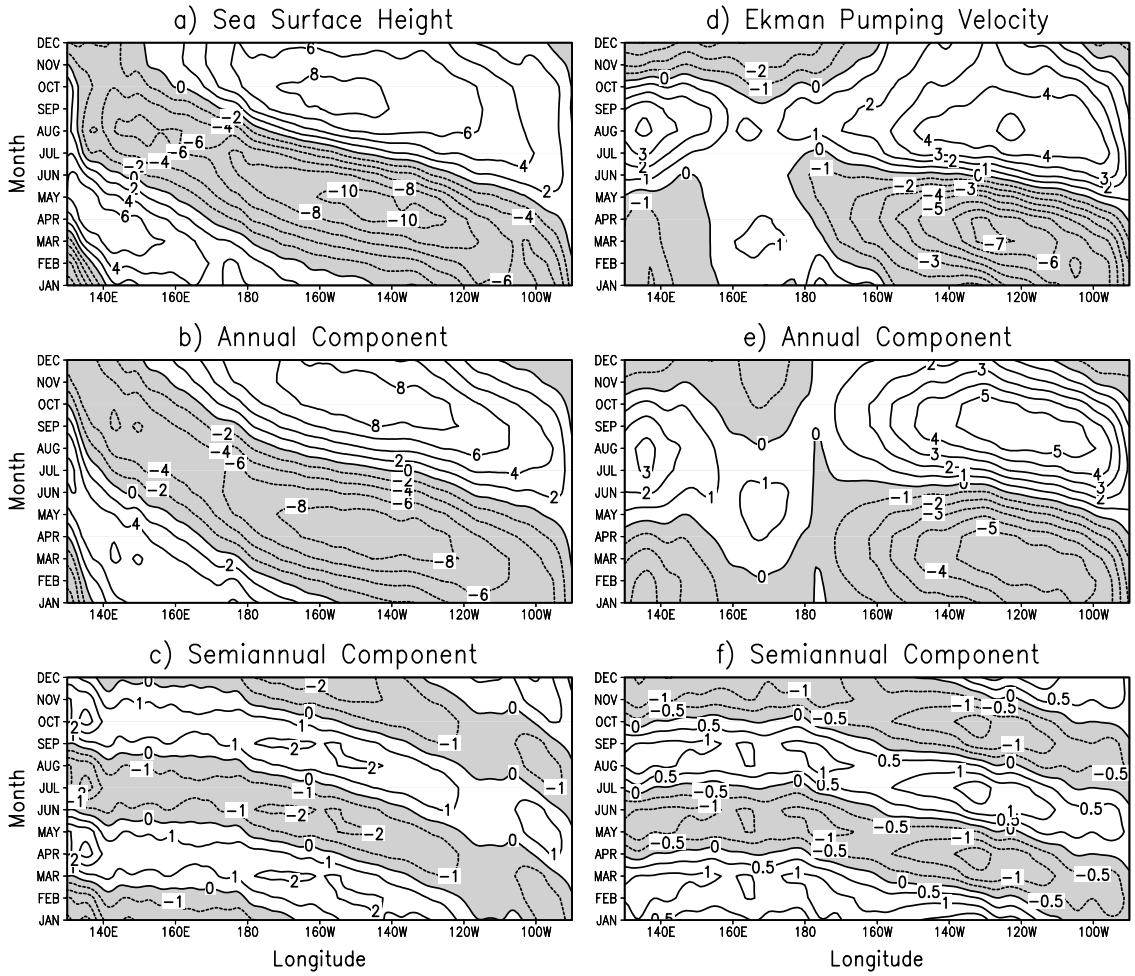

Figure 2. Time-longitude variation and its annual and semiannual components of (left) the merged TOPEX/Poseidon, ERS, and Jason1 sea surface height in cm and (right) the ERS downward Ekman pumping velocity in 10^{-4} cm s^{-1} along 5°N.

then propagate westward until local Ekman pumping changes sign in April/May. The combination of monsoonal wind with westward propagation of Rossby waves is believed to be a key process responsible for the semiannual variation in the western tropical Pacific.

[10] Note that the wave rays do not exactly follow constant latitudes due to the beta-dispersion. As the downwelling Rossby waves propagate westward in the tropical Pacific, they bend slightly toward the equator (Figures 1a and 1b). This leads to a shift of the maximum semiannual variation from 6°–8°N in the eastern tropical Pacific to about 5°N in the western part of the basin. Upon reaching the western boundary, a complex interaction of wave reflection occurs among various islands and topographic features. This, together with local processes forced by the monsoon, generates coastal Kelvin waves propagating southward along the Philippine coast [e.g., *Wang et al.*, 2000]. The westward propagating signal is somewhat distorted in the western tropical Pacific, and the phase speed of semiannual variation is somewhat enhanced (Figure 2b).

3. Response of the Mindanao Current

[11] The MC closes the interior Sverdrup circulation of the tropical gyre in the North Pacific, roughly in the region between 5°N and 13°N near the Philippine coast (Figure 4a). The current is generally geostrophic and driven by a southward directed longshore pressure gradient against friction [e.g., *Qu et al.*, 1998]. As the Rossby waves originating in the central tropical Pacific approach the southern tip of the Philippines, they may alter the longshore pressure gradient that drives the MC, thus resulting in a variation in the current. Because of the complicated topography and the highly variable nature of the current, direct measurements of the MC are very limited. To our best knowledge, the only time series of direct measurement in the MC available so far is from a subsurface mooring system deployed by the Japan Agency for Marine-Earth Science and Technology from October 1999 to July 2002 at 6°50′N, 126°43′E [*Kashino et al.*, 2005]. Analysis of the current measurements from an upward-looking acoustic Doppler current profile (ADCP) clearly demonstrates a semiannual variation in the MC. At 100 m, the ratio of the semiannual versus annual variation is about 8 to 10 (Figure 4b), consistent with our speculation.

[12] To further demonstrate the semiannual variation in the MC, we also examine results from the high-resolution Ocean general circulation model For the Earth Simulator (OFES). This is a nearly global model, with a resolution of 0.1 degree in horizontal and a total of 54 levels in vertical

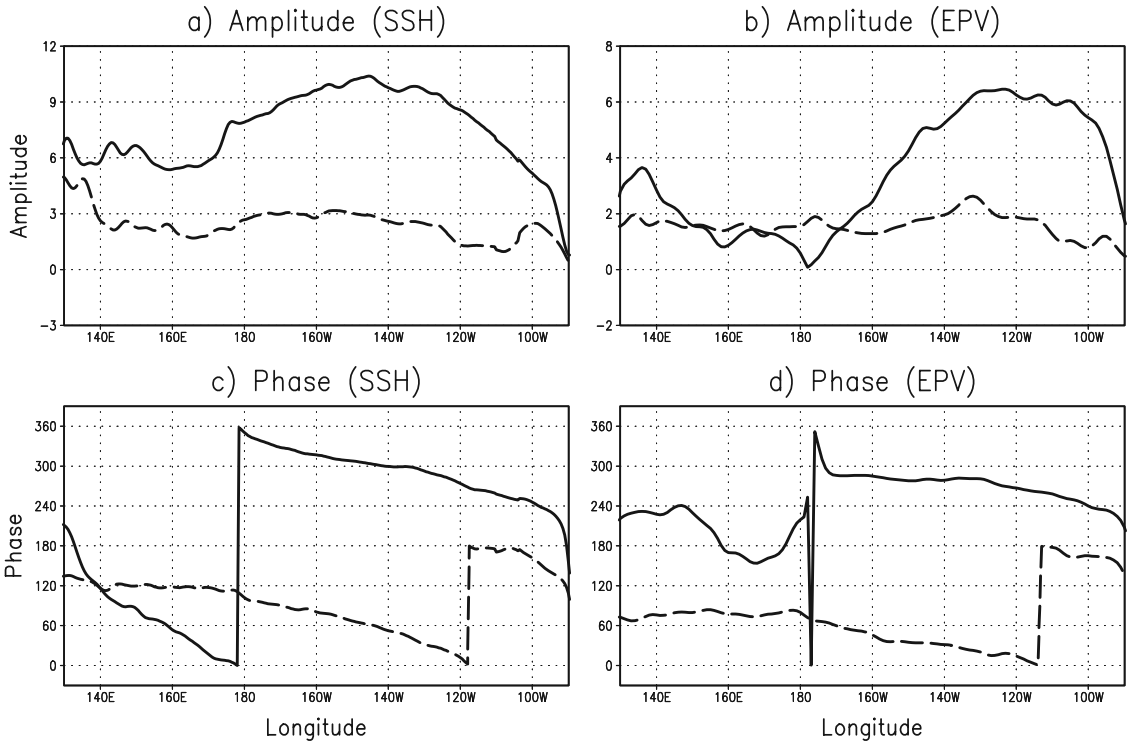

Figure 3. (top) Amplitude and (bottom) phase of annual (solid curves) and semiannual (dashed curves) harmonics of (left) the merged TOPEX/Poseidon, ERS, and Jason1 sea surface height in cm and (right) the ERS downward Ekman pumping velocity in 10^{-4} cm s^{-1} along 5°N.

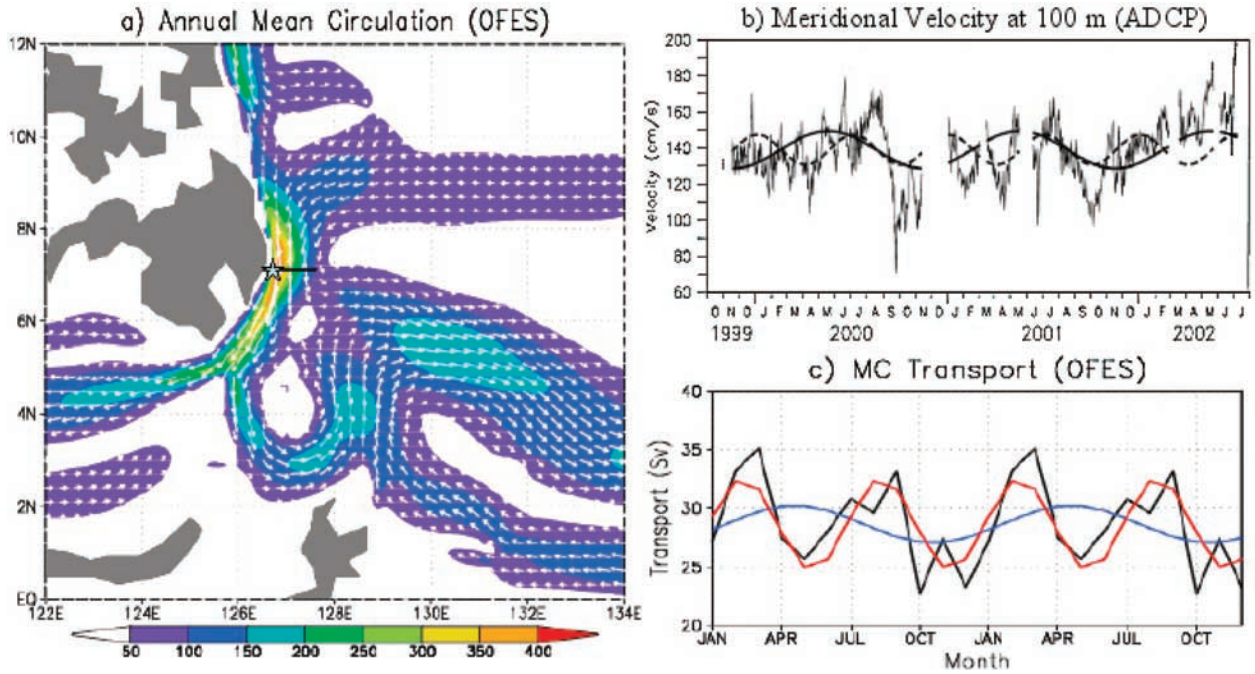

Figure 4. (a) Transport (0–1000 m) per horizontal unit (m^2 s^{-1}) in the western tropical Pacific from OFES, (b) time series of daily averaged velocity (cm s^{-1}) toward 197° true north at 100 m depth at 6°50′N, 126°43′E from ADCP measurements, superimposed with its mean annual and semiannual cycles during the period from October 1999 to July 2002, and (c) seasonal variation of southward Mindanao Current transport (Sv) superimposed with its annual (blue) and semiannual (red) components across 7°N from OFES. The asterisk in Figure 4a indicates the location of ADCP measurements used for Figure 4b and the solid line the location of transaction used for Figure 4c.

[cf. *Masumoto et al.*, 2004]. The model has been able to reproduce most, if not all, of the detailed phenomena observed in the western tropical Pacific (Figure 4a). Along the Philippine coast, the MC intensifies southward and attains its maximum strength at about 7°N, where its transport (0–1000 m) per horizontal unit exceeds 400 m^2 s^{-1}. Integrating this value from the western boundary to 128°E, we obtain an annual mean MC transport of 29 Sv (1 Sv = 10^6 m^3 s^{-1}), in good agreement with earlier observations [e.g., *Toole et al.*, 1990; *Lukas et al.*, 1991; *Qu et al.*, 1998]. Part of the MC turns cyclonically in the Celebes Sea to feed the NECC in the western tropical Pacific, adding to waters that flow directly through the Mindanao Eddy [e.g., *Lukas et al.*, 1991].

[13] The seasonal variation in the MC has been discussed in literature. Based on results from a relatively coarse-resolution model, *Tozuka et al.* [2002] suggests that the MC is strongest in spring and weakest in fall. OFES seems to support this earlier result by showing a maximum transport of 35 Sv in March and a minimum transport of 23 Sv in October (Figure 4c). In addition to the annual variation, OFES also shows a strong semiannual variation in the MC, which has never been reported in literature. At 7°N, 126.8°E, for example, the MC simulated by OFES has two velocity maxima: one in February/March and the other in August/September (figure not shown), in good agreement with the ADCP measurements (Figure 4b). This semiannual signal extends below 500 m, and hence the MC transport (0–1000 m) across 7°N shows a similar semiannual variation as the surface velocity (Figure 4c). This result corresponds well with SSH variation near the southern tip of the Philippines (Figures 2c and 3c). When a forced downwelling (upwelling) Rossby wave arrives along the 4°–6°N wave guide in May/November (February/August), it raises (suppresses) the SSH in the downstream direction of the MC, thus reducing (enhancing) the pressure gradient along the Philippine coast that drives the MC.

4. Discussion

[14] In this study, we report the existence of a previously unexplored semiannual variation in the MC. This semiannual signal is forced by local Ekman pumping combined with the westward propagation of Rossby waves originating in the central tropical Pacific. We speculate that, once these Rossby waves approach the western tropical Pacific, they will affect the sea surface height in the downstream direction of the MC and thus alter the longshore pressure gradient that drives the MC. The prominence of semiannual variation in the MC both from the ADCP measurements and results from OFES confirms this speculation.

[15] Left to be addressed is how local Ekman pumping forced by Monsoon interacts with remotely forced semiannual Rossby waves and how these Rossby waves are reflected and transformed in the western tropical Pacific. Also important for future study is the interannual variation of Rossby waves originating in the central tropical Pacific. With changes in zonal wind stress associated with the migration of ITCZ, one may expect considerable changes in these semiannual Rossby waves, which in turn may induce considerable changes in semiannual variations of the western tropical Pacific. In fact, the year-to-year difference in the MC seasonal variation is obvious during the period of observations from October 1999 to July 2002 (Figure 4b). Further investigation could be provided by completed, long-term sustained observations, as well as continued modeling efforts for the region.

[16] **Acknowledgments.** This research was supported by Japan Agency for Marine-Earth Science and Technology (JAMSTEC) and by National Science Foundation through grant OCE06-23533. Support is also from NASA and NOAA through their sponsorship of the International Pacific Research Center (IPRC) and from Japan Society for Promotion of Science through Grant-in-Aid for Young Scientists (B) 18740291, for Scientific Research (A) 17204040, and for Scientific Research (C) 18540440. The mooring observations were conducted using R/Vs Kaiyo and Mirai under the Tropical Ocean Climate Study project, and the OFES simulations were conducted on the Earth Simulator supported by JASMTEC. The authors are grateful to S. Gao, H. Sasaki, and Y. Shen for constant assistance in processing the satellite data and model output. School of Ocean and Earth Science and Technology (SOEST) contribution 7502, and IPRC contribution IPRC-532.

References

Kashino, Y., E. Firing, P. Hacker, A. Sulaiman, and Lukiyanto (2001), Currents in the Celebes and Maluku seas, *Geophys. Res. Lett.*, *28*, 1263–1266.

Kashino, Y., A. Ishida, and Y. Kuroda (2005), Variability of the Mindanao Current: Mooring observation results, *Geophys. Res. Lett.*, *32*, L18611, doi:10.1029/2005GL023880.

Kessler, W. S. (1990), Observations of long Rossby waves in the northern tropical Pacific, *J. Geophys. Res.*, *95*, 5183–5217.

Kessler, W. S. (2006), The circulation of the eastern tropical Pacific: A review, *Prog. Oceanogr.*, *69*, 181–217.

Lukas, R. (1988), Interannual fluctuations of the Mindanao Current inferred from sea level, *J. Geophys. Res.*, *93*, 6744–6748.

Lukas, R., E. Firing, P. Hacker, P. L. Richardson, C. A. Collins, R. Fine, and R. Gammon (1991), Observations of the Mindanao Current during the Western Equatorial Pacific Ocean Circulation Study (WEPOCS), *J. Geophys. Res.*, *96*, 7098–7104.

Masumoto, Y., and T. Yamagata (1991), Response of the western tropical Pacific to the Asian winter monsoon: The generation of the Mindanao Dome, *J. Phys. Oceanogr.*, *21*, 1386–1398.

Masumoto, Y., et al. (2004), A fifty-year eddy-resolving simulation of the world ocean—Preliminary outcomes of OFES (OGCM for the Earth Simulator), *J. Earth Simulator*, *1*, 35–56.

Meyers, G. (1979), On the annual Rossby wave in the tropical North Pacific Ocean, *J. Phys. Oceanogr.*, *9*, 663–674.

Mitchum, G. T., and R. Lukas (1990), Westward propagation of annual sea level and wind signals in the western Pacific Ocean, *J. Clim.*, *3*, 1102–1110.

Nitani, H. (1972), Beginning of the Kuroshio, in *Kuroshio: Its Physical Aspects*, edited by H. Stommel and K. Yoshida, pp. 129–163, Univ. of Wash. Press, Seattle, Wash.

Qu, T., and R. Lukas (2003), The bifurcation of the North Equatorial Current in the Pacific, *J. Phys. Oceanogr.*, *33*, 5–18.

Qu, T., H. Mitsudera, and T. Yamagata (1998), On the western boundary currents in the Philippine Sea, *J. Geophys. Res.*, *103*, 7537–7548.

Toole, J. M., R. C. Millard, Z. Wang, and S. Pu (1990), Observations of the Pacific North Equatorial Current bifurcation at the Philippine coast, *J. Phys. Oceanogr.*, *20*, 307–318.

Tozuka, T., T. Kagimoto, Y. Masumoto, and T. Yamagata (2002), Simulated multiscale variations in the western tropical Pacific: The Mindanao Dome revisited, *J. Phys. Oceanogr.*, *32*, 1338–1359.

Wang, B., R. Wu, and R. Lukas (2000), Annual adjustment of the thermocline in the tropical Pacific Ocean, *J. Clim.*, *13*, 596–616.

Wijffels, S., E. Firing, and J. Toole (1995), The mean structure and variability of the Mindanao Current at 8°N, *J. Geophys. Res.*, *100*, 18,421–18,435.

J. Gan, Department of Mathematics and Atmospheric, Marine and Coastal Environment Program, Hong Kong University of Science and Technology, Clear Water Bay, Kowloon, Hong Kong, China.

A. Ishida and Y. Kashino, Japan Agency for Marine-Earth Science and Technology, 2-15 Natsushima-cho, Yokosuka, 237-0061, Japan.

T. Qu, IPRC, SOEST, University of Hawai'i at Mānoa, 1680 East-West Road, Honolulu, HI 96822, USA. (tangdong@hawaii.edu)

T. Tozuka, Department of Earth and Planetary Science, Graduate School of Science, University of Tokyo, Tokyo, 113-0033, Japan.